Available online at www.sciencedirect.com

SCIENCE DIRECT®

Journal of the European Ceramic Society 25 (2005) 2599–2602

www.elsevier.com/locate/jeurceramsoc

Conductivity of $La_{0.95}Sr_{0.05}Ga_{0.90}Mg_{0.10}O_{3-\delta}$ obtained by mechanical activation

E. Gomes[a,b,*], M.R. Soares[c], F.M. Figueiredo[a,d], F.M.B. Marques[a]

[a] Department of Ceramics and Glass Engineering, CICECO, University of Aveiro, 3810-193 Aveiro, Portugal
[b] ESTG, Instituto Politécnico de Viana do Castelo, 4900-348 Viana do Castelo, Portugal
[c] Central Lab, University of Aveiro, 3810-193 Aveiro, Portugal
[d] Science and Technology Department, Universidade Aberta, R. da Escola Politécnica 147, 1269-001 Lisbon, Portugal

Abstract

Dense ceramics of $La_{0.95}Sr_{0.05}Ga_{0.90}Mg_{0.10}O_{3-\delta}$ (LSGM) were obtained from La_2O_3, SrO, Ga_2O_3 and MgO precursors activated by dry grinding in a high-energy planetary ball-mill. Samples sintered at 1450 °C for 4 h have an average grain size of ca. 250 nm. This value increases to 5 μm when the sample is annealed for 40 h at the same temperature. Samples prepared by a conventional ceramic route were also obtained with a grain size of 13.5 and 20.5 μm, after sintering at 1550 °C for 4 and 40 h, respectively. Impedance spectroscopy data revealed similar grain conductivities for both materials. However, a significant degradation was observed on ageing the LSGM prepared by the conventional ceramic route, probably due to compositional alterations at the grain boundaries. This degradation was not present in the material prepared from mechanically activated precursors. Grain size effects on the electrical conductivity were analysed to determine the effective grain boundary conductivity and the brick-layer model is assumed to estimate the grain boundary thickness.

Keywords: Milling; Grain boundaries; Electrical conductivity; Lanthanum gallate; Fuel cells

1. Introduction

Feng and Goodenough[1] and Ishihara et al.[2] reported that $LaGaO_3$, when doped with strontium and magnesium ($La_{1-x}Sr_xGa_{1-y}Mg_yO_{3-\alpha}$), exhibit a conductivity several times higher than Y_2O_3-doped ZrO_2, or comparable to that of Gd_2O_3-doped CeO_2, and an ionic transport number close to unity within large ranges of oxygen partial pressure and temperature. Since then, a large amount of work has been dedicated to study these promising solid electrolytes.

Usually, $LaGaO_3$-based electrolytes are obtained via the conventional ceramic route, which implies a high temperature treatment in the range 1400–1600 °C. As a result, these samples have a large particle size and, most importantly, they are chemically inhomogeneous. Small amounts of undesired phases, such as $LaSrGa_3O_7$ and $LaSrGaO_4$, which contribute negatively to the electrical performance, are detected even in materials prepared by chemical solution methods, which can provide products of fine and homogeneous particles.[3–6]

The synthesis via mechanochemical assisted reactions has proven to be versatile to obtain different kinds of materials, namely oxides.[7–9] The high-energy milling makes the activated powder more reactive as a consequence of the fracture of the grains and defects generated during grinding, which leads to a higher internal energy and reduces the thermal barrier for any subsequent reaction.

The aim of this work is to obtain $La_{0.95}Sr_{0.05}Ga_{0.90}Mg_{0.10}O_{3-\delta}$ (LSGM) ceramics by mechanical activation of oxide precursors and compare this material with the LSGM prepared by the conventional solid state route. Differences are discussed based on microstructural and impedance spectroscopy results.

2. Experimental

Powders of $La_{0.95}Sr_{0.05}Ga_{0.90}Mg_{0.10}O_{3-\delta}$ were prepared from high purity lanthanum (Merck), gallium (Aldrich),

---

[*] Corresponding author. Tel.: +351 234 370 263; fax: +351 234 425 300.
E-mail address: framos@cv.ua.pt (E. Gomes).

0955-2219/$ – see front matter © 2005 Elsevier Ltd. All rights reserved.
doi:10.1016/j.jeurceramsoc.2005.03.109

magnesium (Panreac) and strontium oxides. The SrO was obtained from $SrCO_3$ (Merk) calcined at 1100 °C/30 min. Six grams of the oxides were dry grinded in a planetary ball-mill (Retsch Centrifugal Ball-Mill Type S-1/2) using a nylon container and zirconia balls ($Ø = 10$ mm). The ball to powders weight ratio was 10:1. The mechanical activation was performed at $\sim$380 rpm in air during several hours with interruptions, at regular intervals, for cooling and collecting samples for X-ray diffraction analysis (X'Pert MPD Philips, Cu Kα radiation) to monitor structural modifications. A sample from the powder mixture activated for 60 h was also analysed by thermogravimetric (TGA) and differential thermal analyses (DTA), and in situ high temperature X-ray powder diffraction (HTXRD) (Fig. 1).

The information gathered by TGA/DTA and HTXRD was used to design an appropriate sintering curve in order to prepare ceramics in a single thermal treatment at a maximum temperature of 1450 °C for 4 h, with intermediate dwells at 320 °C (2 h), 500 °C (2 h), 700 °C (2 h), 750 °C (25 min) and 900 °C (1 h) for degas.

Ceramics with the same composition were prepared by the conventional ceramic route starting from the same raw materials. The mixture was dried, calcined at 1100 °C for 12 h and again ball-milled and dried. The resultant powder was pressed into pellets and sintered at 1550 °C/4 h with constant heating and cooling rates of 5 K/min. This was the minimum temperature needed to ensure densification ($\geq$93%).

The ceramics prepared by the two methods were characterised by impedance spectroscopy (HP 4284A) at frequencies in the range 20–10^6 Hz with $V_{ac} = 100$ mV. The measurements were carried out in air at temperatures from 200 to 500 °C. The evolution of the spectra was studied in samples annealed at the maximum sintering temperature for 4, 16, 32 and 40 h. Fresh platinum electrodes were applied before every measurement.

Images of the microstructure of the ceramics, thermally etched at a temperature 10% lower than the sintering temperature, were obtained by scanning electron microscopy (SEM) and subsequently analysed using a linear intercept method[10,11] to obtain estimates of the average equivalent grain size.

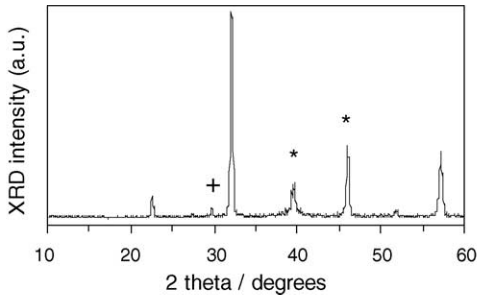

Fig. 1. X-ray diffraction pattern of the activated powders collected in situ at 1200 °C (symbols (+) and (*) identify the secondary $LaSrGa_3O_7$ phase and the platinum from the support, respectively).

3. Results

The XRD data presented in Fig. 1 show that the perovskite is the main phase formed at 1200 °C, although coexisting with a small amount of the usual impurity $LaSrGa_3O_7$;[4,5] the presence of $LaSrGaO_4$, $La_4Ga_2O_9$ or other related phases could not be detected. The fact that the desired perovskite phase was obtained at such low temperature suggests that the mechanochemical approach thus seems promising to improve the processability of these materials.

Dense ceramics (Fig. 2C) could be obtained at a temperature ca. 100 °C lower than that needed to densify samples prepared from non-activated precursors. This is the direct result of avoiding any pre-calcination treatment and of the small size of the activated powders, which is retained up to a maximum average equivalent diameter (G_{av}), ca. 250 nm, when sintering for 4 h (Fig. 2E). A significant increase in G_{av} to $\approx$4.9 μm is noticeable in the ceramics sintered during 40 h (Fig. 2D). It is interesting to note that typical G_{av} values are usually closer to 5–10 μm.[4,5] These are actually closer to values measured for the ceramics obtained via the conventional ceramic route (sintered at 1550 °C for 4 h), as shown by the micrographs in Fig. 2A. The effect on G_{av} (Fig. 2B) is, in this case, less pronounced with G_{av} increasing from 13.5 to 20.5 μm. Besides the larger grain size, a large amount of secondary phase(s) located at the grain boundaries were put into evidence by the thermal etching, as shown in Fig. 2B.

Fig. 3 shows preliminary impedance spectra obtained at 300 °C for the non-activated (A) and activated samples (B) annealed for different periods. The spectra reveal two semicircles, which can be ascribed to the grain interior impedance, at higher frequency, and to the grain boundary, at lower frequency. The grain boundary resistance (R_{gb}) for the activated ceramics (Fig. 3B) is considerably higher than the grain bulk component (R_g), but it decreases to a much lower value after annealing; R_g remains nearly unchanged. The initially high R_{gb} is likely to result from the considerably larger grain boundary density. On the contrary, in the case of conventional ceramics, R_{gb} is clearly lower than R_g (Fig. 3A). Moreover, R_{gb}, and in a smaller measure R_g, increases with increasing grain size. This behaviour may only be explained by a significant alteration of the material at the grain boundaries, probably related to the secondary phases identified in the sample annealed for 40 h (Fig. 2B).

The apparent grain boundary conductivity ($\sigma_{gb,app}$) data, shown in Arrhenius coordinates in Fig. 4, confirm that the aforementioned trend spans over the entire measuring temperature. At least for the activated ceramics, which are expected to have a much higher level of homogeneity, the effect of the grain size on $\sigma_{gb,app}$ may be further analysed in order to obtain estimates of the effective grain boundary conductivity ($\sigma_{gb,eff}$). Since the grain boundary effective area to thickness ratio have opposite effects on the grain boundary capacitance (C_{gb}) and resistance (R_{gb}), the peak relaxation

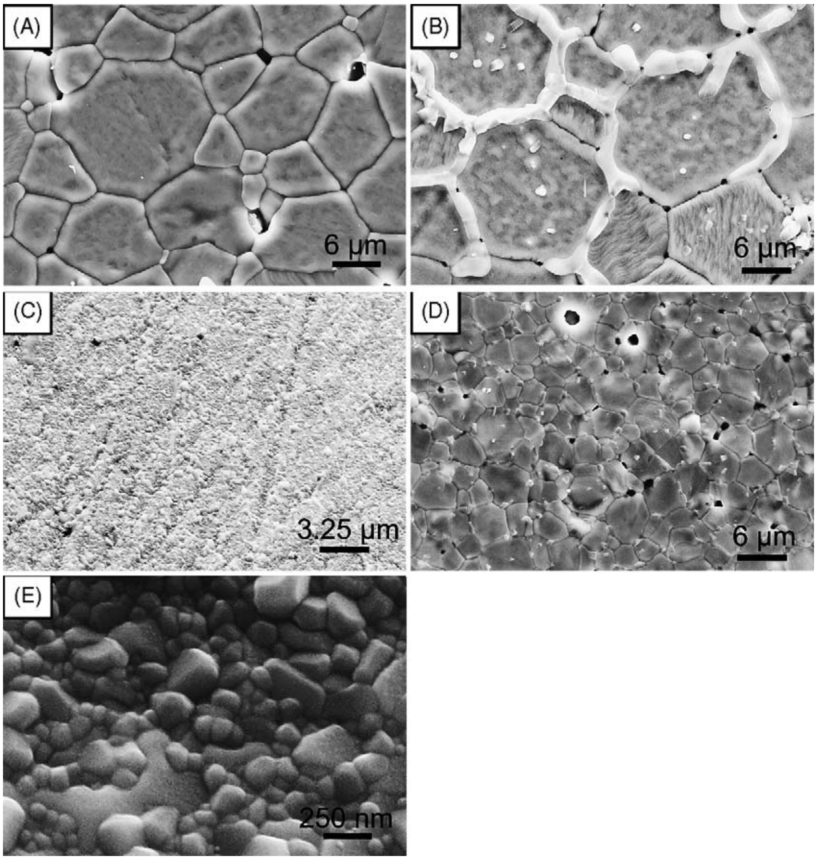

Fig. 2. Scanning electron micrographs of ceramics obtained from non-activated (A and B) and mechanically activated precursors (C–E).

frequency (f_{gb}) is independent of geometry and reads:

$$f_{\mathrm{gb}} = \frac{1}{2\pi C_{\mathrm{gb}} R_{\mathrm{gb}}} = \frac{\sigma_{\mathrm{gb,eff}}}{2\pi \varepsilon_0 \varepsilon_{\mathrm{r}}} \quad (1)$$

where $\varepsilon_0 = 8.854 \times 10^{-12}$ F is the permittivity of vacuum and ε_{r} is the dielectric constant of the bulk. Under these

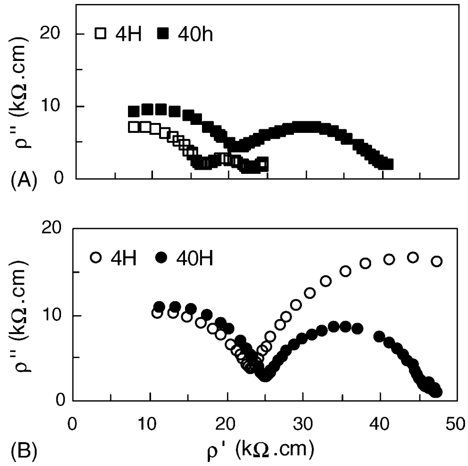

Fig. 3. Impedance spectra collected at 300 °C of conventional (A) and mechanically activated (B) ceramics annealed for different periods of time (frequency decreases from 1 MHz in the first point in the left down to 20 Hz).

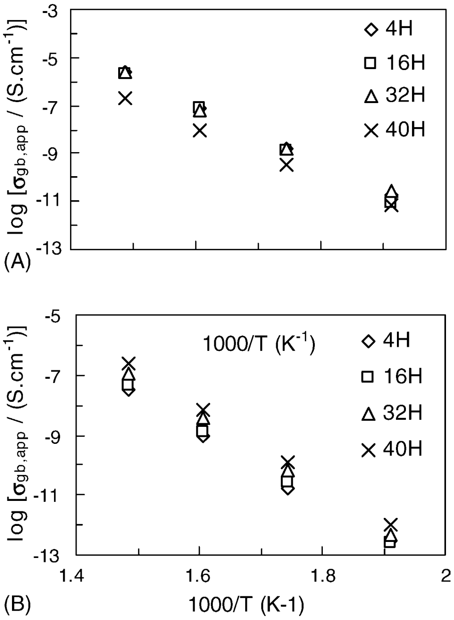

Fig. 4. Temperature dependence of the apparent grain boundary conductivity for ceramics obtained from (A) non-activated and (B) activated ceramics annealed at the maximum sintering temperature for different periods of time.

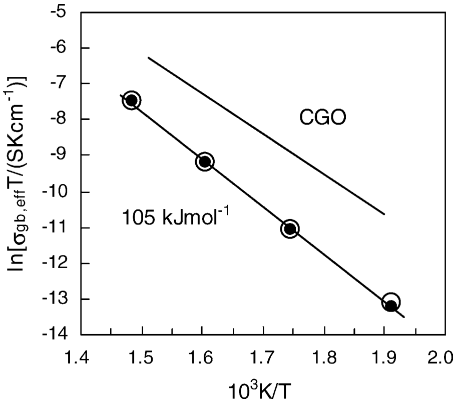

Fig. 5. Temperature dependence of the true grain boundary conductivity for ceramics obtained from mechanically activated precursors sintered for 4 h (○) and 40 h (●) (CGO data taken from reference).[13]

conditions,

$$\sigma_{gb,eff} = 2\pi f_{gb}\varepsilon_0\varepsilon_r. \qquad (2)$$

The $\sigma_{gb,eff}$ estimates shown in Fig. 5 were obtained through Eq. (2) using f_{gb} values extracted from the impedance spectra and $\varepsilon_r = 25$ obtained by others.[12] It can be seen that $\sigma_{gb,eff}$ is slightly lower than estimates obtained for submicrometric Ga-substituted ceria,[13] and, moreover, that it is independent of the grain size. This means that the differences in $\sigma_{gb,app}$ are probably due to a grain size effect. Therefore, by assuming the simplest and well known brick-layer model for the electrical conduction of a polycrystalline ceramic, the grain boundary thickness $\delta_{fg} = G_{av}\sigma_{gb,eff}/\sigma_{gb,app}$ may be estimated to be ≈5 nm, a reasonable value. Nevertheless, the validity of the brick-layer model should be confirmed on data collected from samples with various G_{av} values.

Acknowledgements

This work was supported by FCT, Portugal. Eduarda Gomes would like to thank PRODEP for funding (4/5.3/PRODEP/2000). We also thank Dr. J. Abrantes for making available to us his software for grain size measurements.

References

1. Feng, M. and Goodenough, J. B., A superior oxide-ion electrolyte. *Eur. J. Solid State Inorg. Chem.*, 1994, **31**, 663–672.
2. Ishihara, T., Matsuda, H. and Takita, Y., Doped $LaGaO_3$ perovskite type oxide as a new oxide ionic conductor. *J. Am. Chem. Soc.*, 1994, **116**(9), 3801–3803.
3. Huang, P. and Petric, A., Superior oxygen ion conductivity of lanthanum gallate doped with strontium and magnesium. *J. Electrochem. Soc.*, 1996, **143**(5), 1644–1648.
4. Huang, K., Tichy, R. S. and Goodenough, J. B., Superior perovskite oxide-ion conductor; strontium- and magnesium-doped $LaGaO_3$. II. ac Impedance spectroscopy. *J. Am. Ceram. Soc.*, 1998, **81**(10), 2576–2580.
5. Gorelov, V. P., Bronin, D. I., Sokolova, J. V., Nafe, H. and Aldinger, F., The effect of doping and processing conditions on properties of $La_{1-x}Sr_xGa_{1-y}Mg_yO_3$. *J. Eur. Ceram. Soc.*, 2001, **21**, 2311–2317.
6. Tas, A. C., Majewski, P. J. and Aldinger, F., Chemical preparation of pure and strontium and/or magnesium-doped lanthanum gallate powders. *J. Am. Ceram. Soc.*, 2000, **83**(12), 2954–2960.
7. Mi, G., Saito, F., Suzuki, S. and Waseda, Y., Formation of $CaTiO_3$ by grinding from mixtures of CaO or $Ca(OH)_2$ with anatase or rutile at room temperature. *Powder Technol.*, 1998, **97**(2), 178–182.
8. Zhang, Q. and Saito, F., Mechanochemical synthesis of lanthanum aluminate by grinding lanthanum oxide with transition alumina. *J. Am. Ceram. Soc.*, 2000, **83**(2), 439–441.
9. Algueró, M., Alemany, C., Jiménez, B., Holc, J., Kosec, M. and Pardoet, L., Piezoelectric PMN-PT ceramics from mechanochemically activated precursors. *J. Eur. Ceram. Soc.*, 2004, **24**, 937–940.
10. Anderwood, E. E., *Quantitative Stereology*. Addison-Wesley Publishing Company, Massachusetts, 1970.
11. Mendelson, M. I., Average grain size in polycrystalline ceramics. *J. Am. Ceram. Soc.*, 1969, **42**(8), 443–466.
12. Khan, M. S., Islam, M. S. and Bates, D. R., Dopant substitution and ion migration in the $LaGaO_3$-based oxygen ion conductor. *J. Phys. Chem. B*, 1998, **102**, 3099–3104.
13. Pérez-Coll, D., Núñez, P., Frade, J. R. and Abrantes, J. C. C., Conductivity of CGO and CSO ceramics obtained from freeze-dried precursors. *Electrochim. Acta*, 2004, **48**, 1551–1557.